This paper is published in Engineering Structures Journal

Please cite this article as **Selvaraj, S., Chan, T.-M., & Young, B. (2023). Influence of geometry on failure modes of PFRP single bolted connections. Engineering Structures, 274, 115078, doi: https://oi.org/10.1016/.engstruct.2022.115078**

Highlights

- PFRP plates are tested with single bolt connections.
- Effect of various connection geometries are investigated.
- Evidence for the new combination of failure modes is discussed.
- New parameter for characterising the connection is formulated.
- Directions for the future research is suggested.

Influence of geometry on failure modes of PFRP single bolted connections

Sivaganesh Selvaraj, Tak-Ming Chan* and Ben Young

Department of Civil and Environmental Engineering, The Hong Kong Polytechnic University, Hong Kong, China

*Corresponding author.

Email address: tak-ming.chan@polyu.edu.hk (T.-M. Chan).

Abstract

This paper investigates the ultimate strength, stiffness, and failure modes of pultruded fibre-reinforced polymer (PFRP) single bolted connections subjected to tension. An experimental programme of 72 PFRP connections was conducted. The parameters of the test specimens include plate thickness, bolt diameter, edge distance, end distance and loading angle. A total of 10 different failure modes, including three new combinations of the failure modes were reported. The mechanics reasoning for those new failure modes were discussed. The strength, stiffness and failure modes were interpreted combinedly for determining the effective geometry. The test results were correlated with currently available design guidelines and existing literature for formulating the minimum geometry limitations. A new geometric ratio is proposed for connection characterisation. The appropriateness of the current design standards for minimum geometry is evaluated.

Keywords: PFRP plates; Bolted connections; Structural behaviour; Combined failure modes; Geometric Limitations for design.

1. Introduction

Structures built on/near water create more challenges for engineers than the conventional areas. One of the common problems is the corrosion of steel components in structures which will create

a negative impact on the long-term durability of the structures. An effective solution is to use a fibre-reinforced polymer (FRP) composite (made of basalt, carbon, glass, or fibre with epoxy, polyester, or vinyl ester resin) as a structural material; and it is becoming common in the recent years due to high strength-weight ratio and corrosion resistance. Novel shapes, connection methods, and associated design methods were developed recently [1-9]. Despite the advantages, the practical application of Pultruded FRP (PFRP) structural members is restricted owing to limited research on structural systems with joints. Several studies have been carried out on individual PFRP structural members and reported the applicability for construction; however, some studies on PFRP systems indicated that there are some critical limitations on the connection design and reported the unsatisfactory performance [10-11]. The PFRP systems are connected by bolts; due to their anisotropic material properties; the failure modes of the PFRP connections are critical and govern the design strength. This investigation deals with the physical characteristics of glass PFRP plate single bolted connections.

The main impediment to the wider applicability of the PFRP structures is the unavailability of consistent/reliable design guidelines (CNR 2008; ASCE 2010; EU 2016, and CEN/TS 2020) [12-15], particularly for the minimum requirements for bolting connection geometries. For example, the end distance (e_1) should be equal to 2.5 times the diameter of the bolt (d_b) as per ASCE (2010) [13] and CEN/TS (2020) [15] while the CNR (2008) [12] and EU (2016) [14] recommends $4d_b$. Moreover, the recent experimental research by Martins et al. [16], indicated that the recommendation of the current design codes (CNR 2008; ASCE 2010; EU 2016 and CEN/TS 2020) [12-15] for end distance (e_1) is not adequate, even $4d_b$, as it is leading to undesirable sudden shear out failure. Martins et al. [16] also found that a minimum $8d_b$ end distance is required for achieving bearing failure in PFRP connections. In addition, the current design guidelines have the

inconsistent minimum limitations for the material characteristics for the PFRP plate elements; (i) fibre volume fraction shall not be less than 30% as per ASCE 2010 [13] and 15% as per EU 2016 [14]; (ii) fibres in the longitudinal direction shall not be less than 30% [13]; (iii) fibre orientation: minimum of two directions separated by a minimum of 30 degrees [13].

Even after several comprehensive research by Abd-El-Naby and Hollaway [17], Rosner and Rizkalla [18-19], Turvey and Cooper [20], Prabhakaran et al. [21], Turvey [22], Yuan and Liu [23], Wang [24], Turvey [25], Turvey and Godé [26] and Coelho and Mottram [27], the unavailability of the design specifications indicates the complications involved in the PFRP connection failure interpretation due to variability of material characteristics. Therefore, the design standards for PFRP connections should also include strict and consistent minimum geometric limitations, material characteristics such as fibre orientation, volume/weight fraction, and material properties as a variable rather than specifying the range of material characters. Therefore, single bolt connection tests on PFRP plates were conducted in this investigation. The connection stiffness and strength were correlated with failure modes for achieving minimum geometric limitations.

1.1 Present Investigation

This investigation focused on the structural behaviour and physical characteristics of glass PFRP single bolted connections. In particular, bolted connections in PFRP structures connected by a plated element were investigated for failure mode examination. PFRP plates with a single bolt were tested under tension loading. The parameters which affect the strength and stiffness of the PFRP plates such as fibre orientation (loading angle), the thickness of the PRFP plate, end distance, edge distance, the width of the plate, and diameter of the bolt were investigated. The ultimate load, initial stiffness, bearing stress, and failure modes of the PFRP single bolted connections with respect to the various parameters were reported. The appropriateness of the minimum

requirements for bolt connection geometries in the current guidelines [12-15] and existing literature [16-27] is verified. Finally, some preliminary suggestions for bolt connection geometries of PFRP plates were summarised.

2. Experimental Programme

2.1 Materials

The PFRP plates used in the tests were made from E-glass fibre products manufactured by the Habel Youze FRP company, China. Tensile tests were conducted for longitudinal (0° - member axis/pultrusion direction), transverse (90°), and diagonal (45°) directions of PFRP plates to obtain the mechanical properties. The testing procedures of ASTM D3039/D3039M [28] were followed for the tensile coupon tests and determination of material characteristics such as tensile modulus (E_l), ultimate strength (F_t), and ultimate strain (ε). Tensile coupons were cut from longitudinal (0°), transverse (90°), and diagonal (45°) directions, 4 coupons in each direction. All the coupons had the same dimensions of 250 × 20 mm (length × width) [28-30]. The PFRP coupons were attached to the aluminium tab on both sides at the ends of the coupons for a firm grip during loading. The bond length between the tab and PFRP coupon is according to the minimum suggested bond length described in Section 8.2.2.6 of ASTM D3039/D3039M [28]. The PFRP tensile coupon drawings for the tensile tests are shown in Fig. 1a. The tensile coupon tests were conducted on an Instron universal testing machine. The stress-strain curves obtained from the tensile tests are shown in Figs. 1c-1e. The tensile modulus (E) and ultimate strain (ε) of the PFRP plate were determined using strain readings obtained from the strain gauges attached on both sides of the coupon specimens. The nominal interlaminar shear strength provided by the manufacturer was 25 MPa. The mechanical properties obtained from the PFRP tensile coupons are summarised in Table 1.

115 The fibre weight fraction ratio and layer orientation arrangements of the PFRP were determined
116 using burn-off tests according to ASTM D3171 [31]. The heat treatment was conducted in a
117 furnace with the highest temperature of 500°C ± 5°C for 3 hours. The heat treatment process is as
118 per Selvaraj and Madhavan [32]. The weight of each sample before and after the burn-off test was
119 measured using the digital balance with an accuracy of 0.001 grams. The average fibre weight
120 fraction ratio was found to be 50.56% and 56.86% for 8 mm and 9 mm thick PFRP plates. This is
121 consistent with the existing literature [29, 33, and 34] and according to the minimum requirements
122 of the standards [13-15]. The fibre orientation reinforcement scheme of this PFRP plate is partially
123 symmetric as shown in Fig. 1b; there are bi-directional fibre layers on both the top and bottom
124 sides of the plate and one more bi-directional fibre layer on the mid thickness of the plate but
125 thinner than the top and bottom layers; other fibres are unidirectionally oriented. The fibre layer
126 orientation arrangements were confirmed by weighing the fibres in the direction of pultrusion and
127 bidirectional layer.

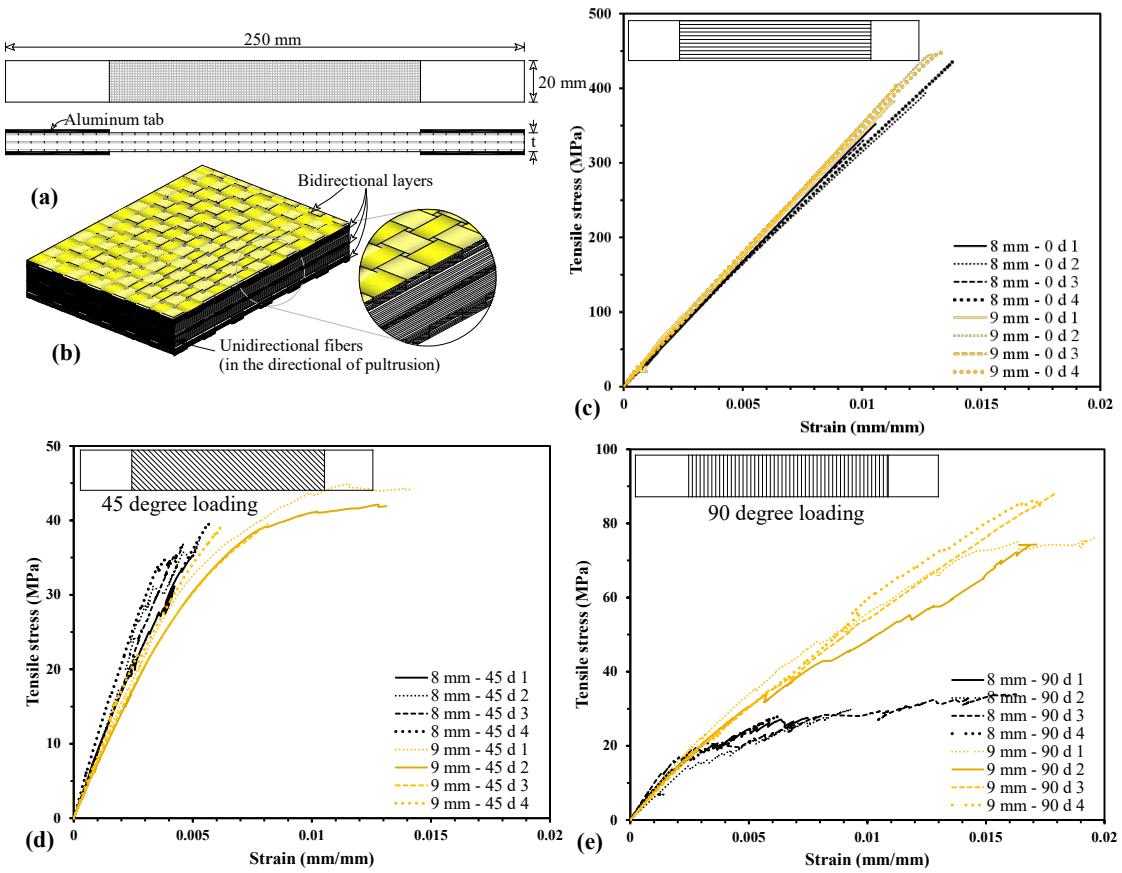

Fig.1. Mechanical properties and fibre architecture of PFRP: (a) Coupon dimensions for the tensile test; (b) Fibre alignment on the PFRP plate determined from burn-off test; (c) Stress-strain curves for 0-degree loading angle corresponding to the direction of pultrusion; (d) Stress-strain curves for 45-degree loading angle corresponding to the direction of pultrusion; (e) Stress-strain curves for 90-degree loading angle corresponding to the direction of pultrusion (labelling "8 mm - 0 d 1" means 8 mm thick PFRP plate loading at 0 degree and sample 1, similarly for others);

Table 1. Material properties of the PFRP plates

Thickness of the PFRP	Sample number	Tensile Modulus (E) (MPa)[a]			Ultimate Strain (ε) % [a]			Ultimate Tensile Strength (F_t) (MPa) [a]		
		0°	45°	90°	0°	45°	90°	0°	45°	90°
8 mm	1	33516	8507	7640	1.06	0.50	0.75	352.0	35.3	27.6
	2	31031	8650	5929	1.27	0.53	0.93	394.5	37.6	29.8
	3	32877	8626	8672	1.01	0.46	1.51	330.0	36.8	33.9
	4	31539	10113	6548	1.38	0.57	0.62	436.8	39.5	27.8
	Mean	32241	8974	7197	1.18	0.51	0.95	378.3	37.3	29.8
	Std Dev	1152.83	761.89	1211.16	0.18	0.05	0.39	47.3	1.7	2.9
	COV	0.04	0.08	0.17	0.15	0.09	0.41	0.12	0.05	0.10
9 mm	1	34705	7640	7646	1.29	1.15	2.46	445.0	44.9	83.0
	2	33535	6886	6780	1.13	1.28	1.71	382.2	42.1	82.8
	3	35293	7264	6625	1.15	0.82	1.80	404.1	39.5	88.4

	4	34141	8401	6855	1.34	0.62	1.71	448.4	39.3	86.1
	Mean	34419	7548	6977	1.23	0.97	1.92	419.9	41.4	85.1
	Std Dev	753.75	646.64	456.56	0.10	0.30	0.36	32.2	2.6	2.7
	COV	0.02	0.09	0.07	0.08	0.31	0.19	0.08	0.06	0.03

Note: The test results E, ε and F_t are summarised with respect to the corresponding angle of loading

2.2 Test Specimen Descriptions

The bolt connection geometric dimensions are shown in Fig. 2, and they affect the strength, stiffness, and failure modes of the connection between the PFRP members. The objective of this test programme is to investigate the various connection geometries to achieve bearing failure in the PFRP bolted connections. Nevertheless, the minimum geometric dimensions suggested in the current design guidelines [12-15 and 35] for FRP were incorporated into the test programme for verifying its appropriateness. The geometric configuration limitations from the design specifications are summarised in Table 2. PFRP plates of thicknesses 8 mm and 9 mm were tested. In each PFRP plate, similar connection geometries were tested to investigate the various end-distance-to-bolt-diameter-ratio (e_1/d_b), plate width-to-bolt-diameter ratio (w/d_b), plate width-to-plate-thickness ratio (w/t) and bolt-diameter-to-plate-thickness ratio (d_b/t). The diameter of the bolt for the PFRP connections should not be less than the thickness of the plate and shall not be more than 1.5 times the thickness of the plate ($t<d_b<1.5t$) in accordance with the current design guidelines. Therefore, the diameter of the bolt for PFRP plates is chosen as 8 mm and 12 mm for 8 mm thick plates and 10 mm and 12 mm for 9 mm thick plates. The bolt hole clearance is kept constant at 1.6 mm for all the bolt diameters for consistency as per ASCE and Strongwell [13 and 35].

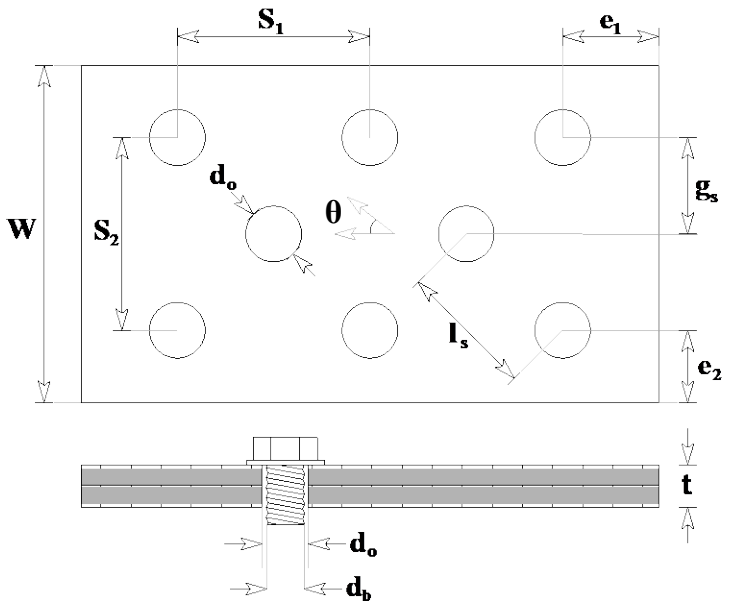

Fig. 2. Bolt connection geometric dimensions

Table 2: Geometric configuration limitations relative to the bolted connections from currently available design codes

Design guidelines	Specified limit	d_b	d_o	e_1	e_2	s_1 and s_2	g_s	l_s
CNR [12]	Min	$\geq t$	d_b	$4d_b$	$0.5S_1$	$4d_b$	-	-
	Max	$\leq 1.5t$	$\geq d_b$+1mm	NLS	NLS	NLS	-	-
ASCE [13]	Min	9.53 *mm*	NLS	$4d_b$[a,d] or $2d_b$[b,c,d]	$1.5d_b$	$4d_b$	$2d_b$	$2.8d_b$
	Max	25.4 mm	d_b+1.6mm	NLS	NLS	$12t$	NLS	NLS
EU [14]	Min	$\geq t$	d_b	$4d_b$	$2d_b$	$4d_b$	$4d_b$	$2.8d_b$
	Max	$\leq 1.5t$	$\geq d_b$+1mm	NLS	NLS	NLS	NLS	NLS
CEN/TS [15]	Min	$\geq t$	d_o-$d_b \leq$ 1mm	30 mm or 2.5 d_b	$2d_b$	$4d_b$	$4d_b$	$2.8d_b$
	Max	$\leq 1.5t$			NLS	NLS	NLS	NLS

Note: [a] - Applicable to a single row of bolts in tensile load; [b] - Applicable to two or three rows of bolts in tensile load; [c] - All connections in compressive load; [d] - Minimum e_1 may be reduced to 2d when the connected member has a perpendicular element attached to the end that the connection force is acting towards; and NLS - No Limit Specified; Refer Fig. 2 for definition of symbols.

The current design guidelines [12-15] suggest that the end distance (e_1) for the PFRP connection shall be a minimum of 2.5 times the diameter of the bolt for achieving bearing failure, despite that several researchers proved that the end distance shall be a minimum of 4 (or more) times the diameter of the bolt to avoid the undesirable shear out failure. Therefore, for investigation, four

different end distances were considered in this study, from $2d_b$ to $8d_b$. The connection geometry and dimensions of the samples are summarised in Table 3. Further, the edge distance (e_2) is varied from $1.5d_b$ to $2d_b$ for each end distance (e_1) limit. For all the above connection geometries (ratios e_1/d_b, w/d_b, w/t, and d_b/t), the angle of loading is varied with respect to the direction of pultrusion. Three different loading angles were studied, 0 degrees (member longitudinal axis/pultrusion direction), 90 degrees (transverse), and 45 degrees (diagonal) totaling 72 test samples. The nomenclature of the test specimen is as follows: thickness of the PFRP plate (t) / diameter of the bolt (d_b) / end distance (e_1) / edge distance (e_2) / angle of loading; for example, 8/8/2db/1.5db/0°.

Table 3. Specimen dimensions and test results of PFRP single bolted connections

Specimen nomenclature	(w/t) / (e_1/d_b)	Initial Stiffness (kN/mm)	Maximum Load (F) (kN)	Bearing stress (F_{br}) (MPa)	Failure mode
8/8/2db/1.5db/0	1.50	4.23	5.32	83.16	CL
8/8/2db/1.5db/45	1.50	3.45	4.76	74.39	NT 45
8/8/2db/1.5db/90	1.50	2.95	2.22	34.74	TS
8/8/2db/2db/0	2.00	5.63	6.52	101.94	SO
8/8/2db/2db/45	2.00	4.37	5.57	86.97	NT 45
8/8/2db/2db/90	2.00	3.11	3.58	55.86	TS
8/8/4db/1.5db/0	0.75	5.22	12.14	189.63	CL
8/8/4db/1.5db/45	0.75	4.47	4.23	66.02	NT 45
8/8/4db/1.5db/90	0.75	3.33	2.92	45.59	TS
8/8/4db/2db/0	1.00	5.09	13.58	212.25	SO
8/8/4db/2db/45	1.00	4.31	8.12	126.92	NT 45
8/8/4db/2db/90	1.00	3.43	3.91	61.02	TS
8/8/6db/2db/0	0.67	5.51	14.22	222.24	LS
8/8/6db/2db/45	0.67	4.25	6.79	106.10	NT 45
8/8/6db/2db/90	0.67	4.10	4.26	66.57	TS
8/8/8db/2db/0	0.50	6.14	17.42	272.13	B+LS
8/8/8db/2db/45	0.50	4.91	5.58	87.23	NT 45
8/8/8db/2db/90	0.50	4.09	4.71	73.65	TS
8/12/2db/1.5db/0	2.25	5.63	9.41	98.06	CL
8/12/2db/1.5db/45	2.25	3.64	6.59	68.65	NT 45
8/12/2db/1.5db/90	2.25	3.39	4.47	46.58	TS
8/12/2db/2db/0	3.00	5.84	9.56	99.61	SO
8/12/2db/2db/45	3.00	4.92	8.32	86.66	NT 45

8/12/2db/2db/90	3.00	3.60	5.63	58.67	TS
8/12/4db/1.5db/0	1.13	5.64	18.13	188.83	CL
8/12/4db/1.5db/45	1.13	5.09	6.50	67.74	NT 45
8/12/4db/1.5db/90	1.13	4.06	3.58	37.31	TS
8/12/4db/2db/0	1.50	5.43	19.73	205.53	SO
8/12/4db/2db/45	1.50	5.14	10.36	107.87	NT 45
8/12/4db/2db/90	1.50	4.17	5.07	52.81	TS
8/12/6db/2db/0	1.00	6.79	23.34	243.11	B+LS
8/12/6db/2db/45	1.00	5.63	9.91	103.22	NT 45
8/12/6db/2db/90	1.00	5.46	5.67	59.06	TS
8/12/8db/2db/0	0.75	6.84	24.27	252.80	B+SO
8/12/8db/2db/45	0.75	5.65	8.95	93.21	NT 45
8/12/8db/2db/90	0.75	5.64	6.23	64.86	TS
9/10/2db/1.5db/0	1.67	6.01	10.30	114.43	CL
9/10/2db/1.5db/45	1.67	4.78	7.80	86.71	NT 45
9/10/2db/1.5db/90	1.67	3.68	8.36	92.92	DL+TS
9/10/2db/2db/0	2.22	5.64	10.90	121.12	SO
9/10/2db/2db/45	2.22	4.61	8.61	95.62	NT 45
9/10/2db/2db/90	2.22	4.99	9.79	108.82	DL+TS
9/10/4db/1.5db/0	0.83	5.67	19.73	219.26	CL
9/10/4db/1.5db/45	0.83	4.75	6.84	76.02	NT 45
9/10/4db/1.5db/90	0.83	4.26	10.00	111.06	DL+TS
9/10/4db/2db/0	1.11	6.77	22.00	244.41	SO
9/10/4db/2db/45	1.11	5.18	12.20	135.58	NT 45
9/10/4db/2db/90	1.11	4.18	10.99	122.16	DL+TS
9/10/6db/2db/0	0.74	6.98	23.38	259.82	B+SO
9/10/6db/2db/45	0.74	5.02	11.08	123.16	NT 45
9/10/6db/2db/90	0.74	4.49	13.23	147.00	DL+TS
9/10/8db/2db/0	0.56	6.99	23.39	259.94	DL+PB
9/10/8db/2db/45	0.56	5.00	11.11	123.44	NT 45
9/10/8db/2db/90	0.56	4.48	10.68	118.63	DL+TS
9/12/2db/1.5db/0	2.00	6.47	13.66	126.52	CL
9/12/2db/1.5db/45	2.00	3.77	9.23	85.49	NT 45
9/12/2db/1.5db/90	2.00	3.92	10.02	92.75	DL+TS
9/12/2db/2db/0	2.67	5.52	13.51	125.07	SO
9/12/2db/2db/45	2.67	4.24	10.05	93.06	NT 45
9/12/2db/2db/90	2.67	4.40	11.81	109.38	DL+TS
9/12/4db/1.5db/0	1.00	6.71	18.66	172.74	CL
9/12/4db/1.5db/45	1.00	5.25	8.28	76.68	NT 45
9/12/4db/1.5db/90	1.00	4.63	10.77	99.77	DL+TS
9/12/4db/2db/0	1.33	6.33	23.96	221.88	DL+PB
9/12/4db/2db/45	1.33	4.25	14.79	136.90	NT 45
9/12/4db/2db/90	1.33	5.30	13.79	127.72	DL+TS
9/12/6db/2db/0	0.89	6.55	30.15	279.20	DL+PB
9/12/6db/2db/45	0.89	5.61	13.90	128.68	NT 45

9/12/6db/2db/90	0.89	4.22	13.83	128.06	DL+TS
9/12/8db/2db/0	0.67	7.57	30.63	283.63	B
9/12/8db/2db/45	0.67	6.10	14.28	132.22	NT 45
9/12/8db/2db/90	0.67	4.65	13.53	125.29	DL+TS

B - Bearing; CL - Cleavage tension; DL - Delamination; NT 45 - Net tension at 45 degrees; PB - Partial Bearing; SO - Shear-out; LS - Longitudinal Splitting; TS - Transverse Split

2.3 Experimental test setup

The tensile test on PFRP plate single bolted connections is carried out using an Instron Universal Testing machine. The length of the test sample is 160 mm and the width of the PFRP plate is decided based on the edge distance (e_2) as shown in Fig. 3a. One end of the PFRP plate is attached with aluminium plates on both sides for a bond length of 50 mm to grip with the universal testing machine. The test setup is shown in Fig. 3b. The test setup is developed such that the bolt is pulled by the steel plates from either of the sides and the failure will occur only on the FRP plate. The tensile load was applied at a constant displacement rate of 0.8 mm/minute. The loading was applied until the failure of the FRP plate. The fully threaded stainless-steel rods were used for simulating the bolts in the FRP connections. In the conventional PFRP connections, the connecting components, for example, the web cleats are laterally restrained by a beam on one side and free on the other side, however, in the present investigation the PFRP plates were tested without any lateral constraints so that the failure mode can freely occur. Furthermore, the tightening of the bolt with torque may lead to crushing of the PFRP plate, therefore, to eliminate the influence of torque and washer on failure modes, the threaded rods were not tightened with the PFRP plates [27 and 36].

3. Test results

The failure modes, ultimate load, initial stiffness, and bearing stress of the PFRP single bolted connections are summarised in Table 3 and Figs. 4-6. According to the current design guidelines

[12-15] and the existing literature [23-27 and 36], the PFRP plates were generally subjected to four different failure modes, namely net tension, shear-out, bearing, and cleavage tension. However, in the present investigation, both distinctive (individual failure mode) and new combinations of failure modes were observed. In some cases, the failure mode has changed after the load drop (in the load-displacement plot) at the end of the loading curve; such failure modes were also considered distinctive. The failure mode is termed as combined only when two failure modes have occurred simultaneously. A new distinctive failure mode called longitudinal splitting (LS-sudden longitudinal crack from the edge of the bolt hole to the plate end) of the PFRP plate was observed. In the present investigation, a total of ten different failure modes were observed in PFRP single bolted connections as shown in Fig. 4. Out of the ten failure modes, four of them were interactive/combination of two failure modes. The term ultimate load (kN) means, the peak strength value in the load versus displacement graph [16]. The initial stiffness (kN/mm) means the initial slope of the load versus displacement graph. The deformation of the bolt hole in the connection is used in the load versus displacement graphs in Figs. 5a and 5d. Based on the literature [27] and design guidelines [12-15], the criterions used for classifying the failure modes are: (i) bearing - large deformation (progressive) parallel to the loading direction; (ii) splitting - longitudinal crack from the edge of the hole to the plate end; (iii) shear-out - caused by shear stresses and occurs along shear-out planes on the hole boundary in the loading direction; (iv) net tension - crack propagations transverse to the loading direction; (v) cleavage tension – a combination of net tension and shear-out failure; (vi) transverse split - almost same as net tension but happens in 90 degree fibre loading; (vii) delamination - separation of top and bottom bi-directional layer in the PFRP plate. The failure modes observed in the present investigation and the mechanics reasoning for them are described in the following sections.

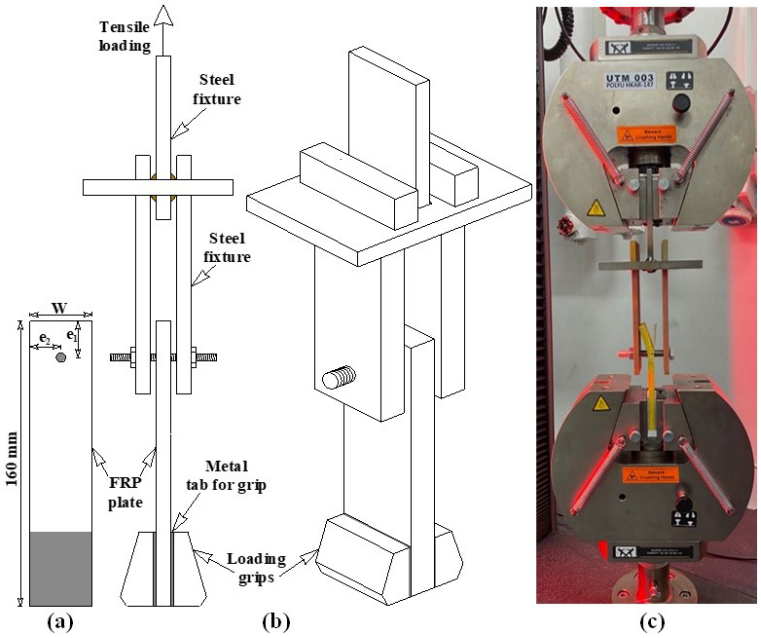

Fig. 3. (a) Dimensions of the test sample; (b-c) Test setup for single bolt connection test

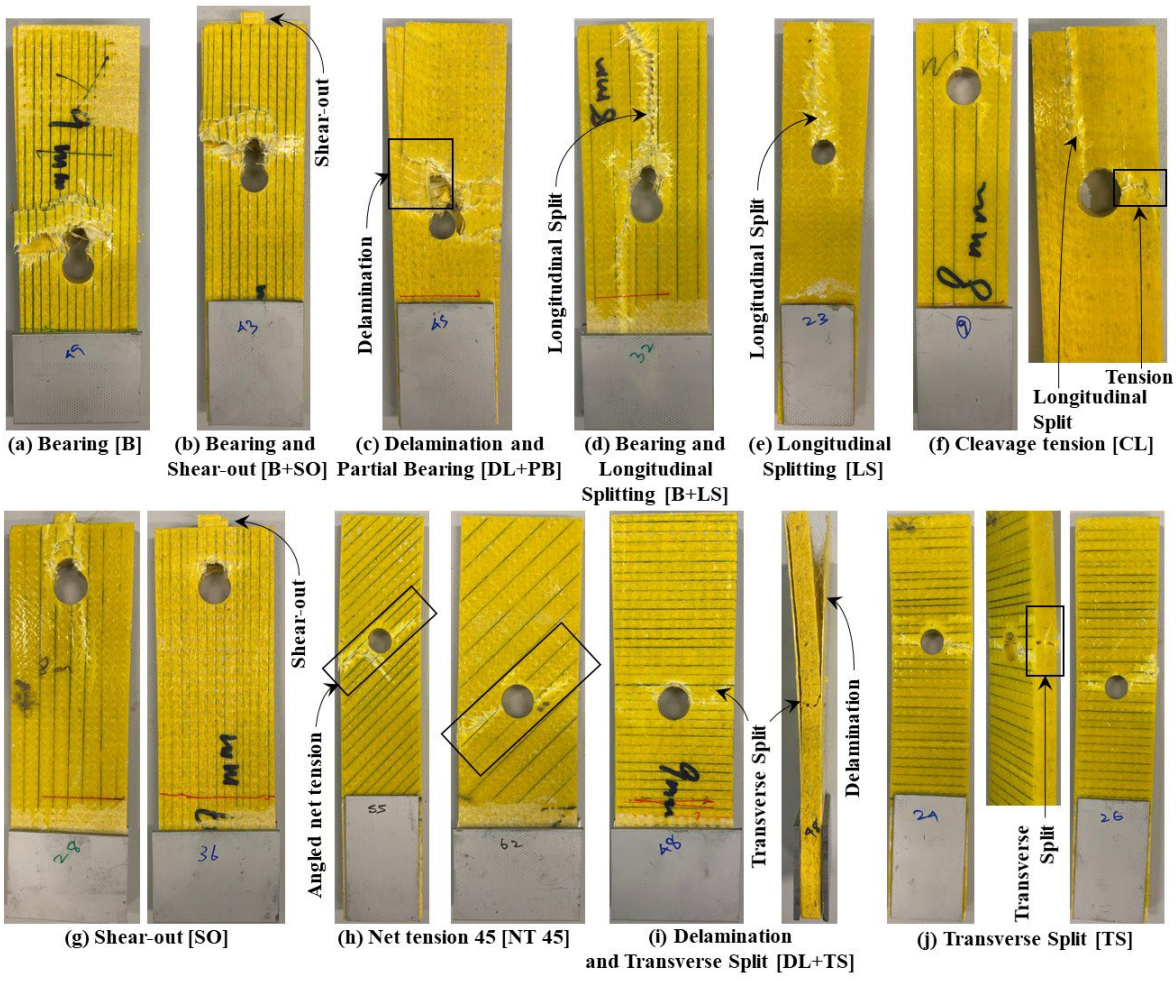

Fig. 4. Various failure modes were observed in the PFRP single bolted connection tests

3.1 Combined failure modes in PFRP connections

Four of the failure modes observed from the present PFRP bolted connection tests were a combination of two individual failure modes due to the material and fibre orientation characteristics. One of the combined failure modes was bearing and shear-out which was observed in the previous investigation [36] as well. In the bearing and shear-out combination failure (B+SO see Fig. 4b), the bearing occurs first and then the shear-out occurs followed by a sudden load drop. The conventional cleavage failure mode is also a combination of shear-out and net-tension; however, three new combination failure modes were observed in the present investigation. Those new combined failure modes were delamination and partial bearing (DL+PB see Fig. 4c), bearing and longitudinal splitting (B+LS see Fig. 4d), and delamination and transverse split (DL+TS see Fig. 4i). The reasoning for the three combined failure modes is given as follows.

Delamination and partial bearing (DL+PB): The delamination (in other words, it can be noted as a net tension failure of a top and bottom bi-directional layer in the FRP plate followed by layer debonding) and bearing occur simultaneously, then the delamination extended along the full length of the member with the increase in bearing as shown in Fig. 4c. The delamination is between the bidirectional layer and fibres oriented in the direction of pultrusion. The delamination failure is perhaps attributed to inadequate thickness and bonding of the top and bottom bi-directional layers. This delamination and partial bearing failure occurred in the specimens with less than 80 mm end distance of 9 mm thick PFRP plates (specimens 9/10/8db/2db/0 with 80 mm edge distance, 9/12/4db/2db/0 with 48 mm edge distance, and 9/12/6db/2db/0 with 72 mm edge distance - Table 3). Although it is a combination of bearing, this failure mode should be regarded as an undesirable failure mode as the delamination is propagating for an entire length or width of the PFRP element leading to a reduction of thickness. The reduction of thickness for a portion of the PFRP element

may certainly lead to a sudden collapse of the entire structure. To avoid this failure mode, the thickness of the bi-directional layer on the top and bottom sides of the PFRP may be increased. The minimum thickness limitation for this bi-directional layer may be included in the design guidelines after further research to avoid delamination failure.

Bearing and longitudinal splitting (B+LS): Bearing and longitudinal splitting failure mode is again an undesirable failure mode, though it is a combination of bearing. The splitting of the PFRP plate began to occur with small bearing deformation as shown in Fig. 4d. The longitudinal splitting failure with a combination of bearing occurred only in 8mm thick PFRP plates (8/8/8db/2db/0 - 64 mm end distance and 8/12/6db/2db/0 - 72 mm end distance - see Table 3), and may be attributed to the inadequate width of the PFRP plate resulting from edge distance ($2d_b$) to distribute the force and thickness of the bidirectional layers. The top and bottom bi-directional layers were not sufficiently confining the unidirectional fibres from splitting. It should be noted that the PFRP plate connection with an end distance of 96 mm ($8d_b$) (8/12/8db/2db/0) did not fail in longitudinal splitting failure, but failed in bearing and shear out failure with higher deformation of 15.6 mm (Figs. 5a and 5c). This indicates that the inadequate confining effect of the bidirectional layer as a result of less thickness necessitates a larger end distance (e_1) up to $8d_b$ to overcome the longitudinal splitting failure and achieve bearing failure.

Delamination and transverse split (DL+TS): The transfer split is obvious due to the angle of loading (90 degrees perpendicular to the pultrusion direction) but the combination of delamination throughout the length (as shown in Fig. 4i) once again indicates that the inadequacy of the fibre orientation pattern particularly the bonding between unidirectional fibres and bidirectional layers. It should also be noted that the delamination and transverse split combined failure occurred only in all the 9 mm thick PFRP plates (12 specimens with 90-degree loading – Figs. 4i, 5e, and 5f)

while the 8 mm thick plates with similar geometry configuration failed in distinctive transverse split (12 specimens) failure as shown in Figures 4i and 4j and Table 3. This indicates that the thickness of the top and bottom bidirectional layers on the PFRP plates should be increased with an increase in the overall thickness (t) of the plate. The design specifications may suggest the ratio of the thickness of the bidirectional layer to the total thickness (t) rather than the percentage of fibre in the longitudinal direction alone [13].

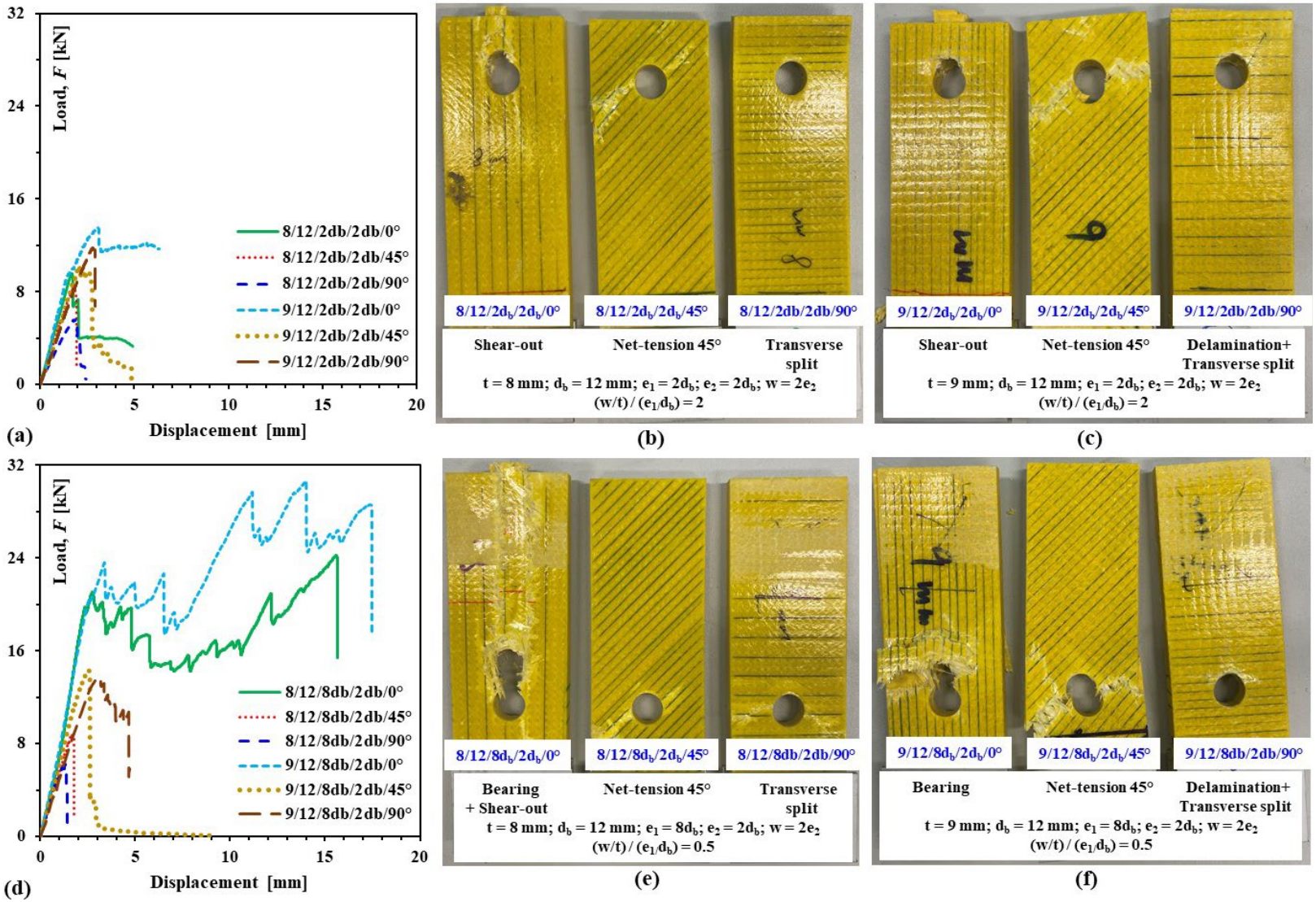

Fig. 5. Response of PFRP plate for different angles of loading with respect to the direction of pultrusion: (a) Load-displacement response with $2d_b$ end distance; (b-c) Failure modes of PFRP plates with $2d_b$ end distance; (d) Load-displacement response with $8d_b$ end distance; (e-f) Failure modes of PFRP plates with $8d_b$ end distance.

The above observations and interpretations pertaining to the combined failure modes of PFRP connections indicate that the material characteristic limitations such as fibre orientation, and thickness of the bi-directional layers or percentage of fibres in transverse direction shall be included as a variable in conjunction with the minimum geometric dimension requirement for connection.

3.2 Influence of geometric dimensions on the structural behaviour of connections

3.2.1 Effect of edge distance (e_2)

An adequate edge distance (e_2) is required with a combination of other geometric dimensions to overcome the undesirable failure and to achieve the failure mode which can exhibit larger deformation (warning) before ultimate failure. Two different edge distances (e_2) were used in the present study as per the current design guidelines; (i) 1.5 times the diameter of the bolt as per ASCE [13]; (ii) 2 times the diameter of the bolt as per CNR 2008, EU 2016 and CEN/TS 2020 [12,14 and 15]. The variation in edge distance was studied with two PFRP plate thicknesses (t), two different bolt diameters (d_b), two end distances ($e_1 = 2d_b$ and $4d_b$), and three different loading angles. The failure mode of the PFRP plate single bolted connections for an edge distance of $1.5d_b$ is cleavage failure (CL) which has been changed to shear-out (SO) failure after increasing the edge distance to $2d_b$. This indicates that the $1.5d_b$ edge distance was insufficient to distribute the load and led to net tension failure on one side of the bolt as shown in Fig. 4f in all the variable parameters. This change in failure mode from cleavage to shear-out increased the ultimate loading capacity of the single bolted connection with a range of 11.5% (compare 9/10/4db/2db/0 and 9/10/4db/1.5db/0 in Table 3) to 28.4% (compare 9/12/4db/2db/0 and 9/12/4db/1.5db/0 in Table 3). Based on this observation, the rest of the specimens with higher-end distances ($6d_b$ and $8d_b$) were tested with $2d_b$ edge distances.

3.2.2 Effect of angle of loading with respect to the direction of pultrusion

The influence of fibre orientation with respect to the angle of loading is an important parameter for the structural behaviour of PFRP members, particularly for the connections as members are connected from various angles. In the test programmme, test parameters of the PFRP specimens (e_1, e_2, d_b, t) were kept constant and only the angle of loading is changed (0 degree, 45 degree and 90 degree) for comparing the test results. The results indicated that loading parallel to the direction of pultrusion (0 degree) had the highest stiffness and ultimate load compared to 45 degree and 90 degree loading as shown in Figs. 5a and 5d. To be precise, the difference in stiffness between the specimens of 45 degree and 90 degree with respect to 0 degree is 15.1% (compare 8/12/2db/2db/0 with 8/12/2db/2db/45 in Table 3) and 38.4% (compare 8/12/2db/2db/0 with 8/12/2db/2db/90 in Table 3). This difference in stiffness with respect to the angle of loading did not change much even after increasing the end distance (e_1) from $2d_b$ to $8d_b$. This indifference in stiffness even after increasing the end distance to $8d_b$ is perhaps due to the fact that stiffness typically depends on the bearing thickness of the material. However, there is a significant difference between the ultimate load of the bolted connections with corresponds to the change in angle of loading and increase in end distance from $2d_b$ to $8d_b$ as shown in Table 3. The significant increase in ultimate load after changing the edge distance may be attributed to the presence of longitudinal fibre in the direction of loading. It should be noted from Table 3 that for some specimens in 9 mm thick PFRP plate, the 90 degree loading had a higher ultimate load and initial stiffness compared to the 45 degree loading, this may be attributed to the change in failure mode from transverse split (TS) (8 mm plate) to a combination of delamination and transverse split (DL+TS) in 9 mm plate. A more detailed discussion about the increase in ultimate load with respect to the increase in end distance (e_1) is discussed in the following sections of this paper.

The failure modes are also changed after changing the angle of loading as shown in Fig. 5. All the specimens with 45 degree and 90 degree loading failed in net tension, transverse split, and delamination, which were typically regarded as undesirable failure modes for PFRP connections. While the specimens with the angle of loading parallel to the direction of pultrusion (0 degree) have a desirable failure mode (bearing) when adequate end distance ($\geq 8d_b$) is provided. The previous investigations [18] with the same parameters indicated that the change in angle of loading also varied the failure mode, but the pattern of the loading curve remains the same. However, in the present study, the pattern of the loading curve also changed concerning the change in failure mode as shown in Fig. 5a and 5d. The load-displacement curves of the 45 degree and 90 degree specimens were linear till the ultimate load and sudden drop of more than 50%, whereas for the 0 degree, the load drop is not significant and with adequate end distance (Fig. 5 d - 8/12/8db/2db/0° versus 8/12/8db/2db/45° and 8/12/8db/2db/90°). The load-displacement curve of a 0 degree specimen is initially linear, followed by a markedly non-linear pattern with successive small load reductions and increases until reaching 15 mm of displacement (see curves 8/12/8db/2db/0° and 9/12/8db/2db/0° in Fig. 5d). The non-linear loading curve with resistance for a displacement magnitude (15 mm) higher than the diameter of the bolt is considered to be the desired failure mode as it shows a warning before ultimate failure.

3.2.3 Effect of end distance (e_1) in combination with plate width (w)

To analyse the variation of failure mode and ultimate load with regards to the end distance, the failure loads of the connections were compared with the e_1/d_b ratio in Fig. 6. This was compared for two different bolt diameters in two different thicknesses of the PFRP plates. The comparison indicates that the strength of the connection did not increase significantly after $4d_b$ and up to $8d_b$, but the failure mode, improved from brittle nature to progressive damage with an adequate warning

353 sign. To quote precisely, only specimens with an end distance of $8d_b$ had failed in bearing failure
354 or in combination with bearing failure as shown in Figs. 6e-6h. Nevertheless, no meaningful
355 conclusion can be drawn based on the comparison of the e_1/d_b ratio and ultimate load for the overall
356 connection geometric dimensions due to the presence of various parameters.

357 The PFRP connections should have a progressive failure and exhibit prior warning before ultimate
358 failure; to achieve this, the connecting element should have an adequate width, thickness, and
359 deformable distance along the direction of loading. Existing literature indicates that the end
360 distance and width of the plate are the most influential factor that determines the failure modes of
361 the PFRP connections. However, various literature has suggested different limits of end distance
362 (e_1) for achieving progressive damage growth with prior warning to failure. To be specific, Rosner
363 and Rizkalla [18] suggested an e_1/d_b ratio of 5, Lee et al [36] suggested an e_1/d_b ratio of 4, and the
364 comprehensive review article by Coelho and Mottram [27] suggested that the e_1/d_b ratio of 5 with
365 w/d_b ratio of 7. More recently, the latest experimental research article by Martins et al [16] found
366 that the e_1/d_b ratio beyond 8 exhibited bearing failure with a warning of 15 mm (average)
367 deformation along the loading direction. These inconsistent conclusions from various articles
368 pertaining to the end distance (e_1) impede the development of reliable design specifications for
369 PFRP structures.

370

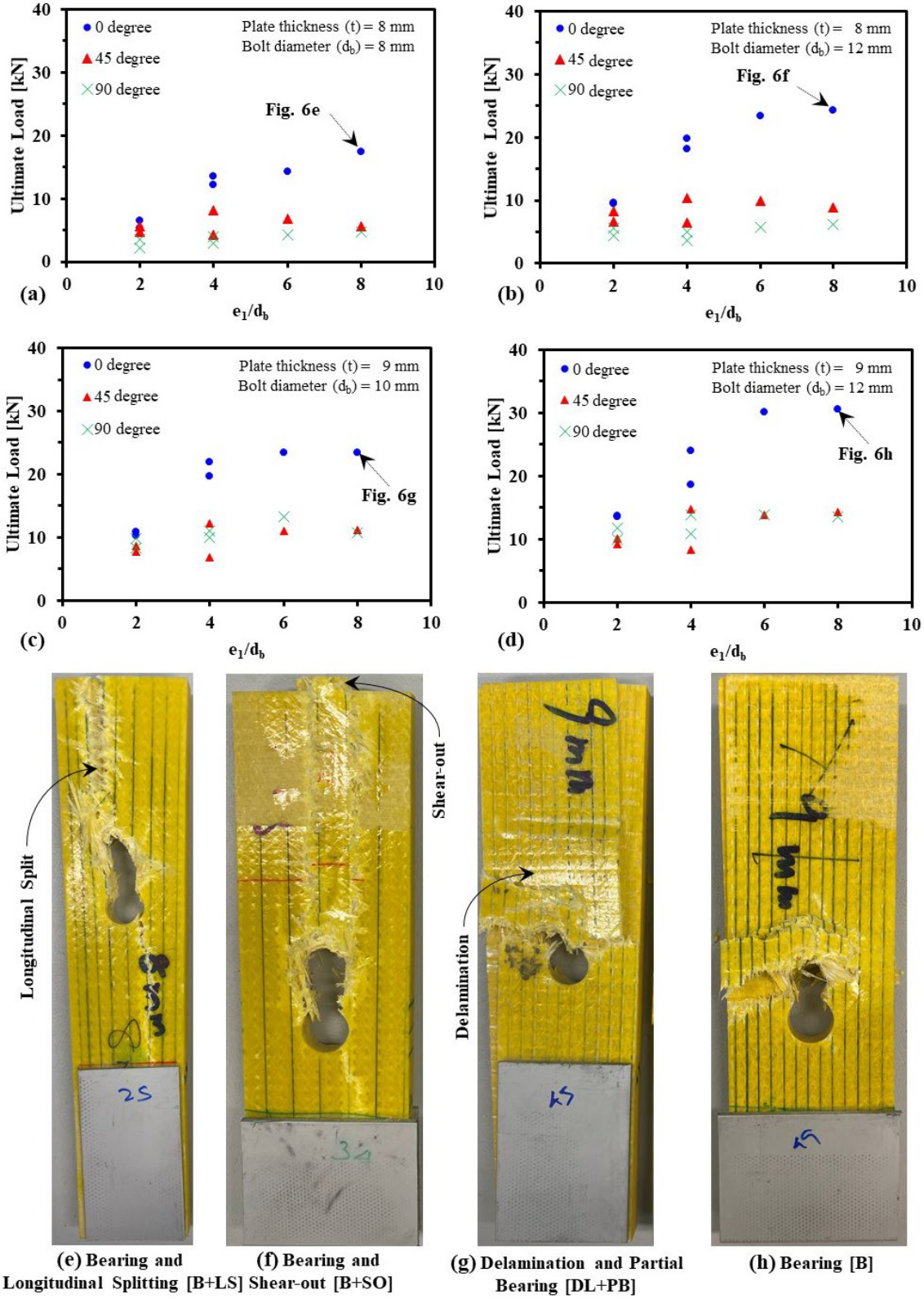

Fig. 6. Response of PFRP plate for different end distances from $2d_b$ to $8d_b$: (a) Load versus e_1/d_b response for 8 mm plate and 8 mm bolt diameter; (b) Load versus e_1/d_b response for 8 mm plate and 12 mm bolt diameter; (c) Load versus e_1/d_b response for 9 mm plate and 10 mm bolt diameter;

375 (d) Load versus e_1/d_b response for 9 mm plate and 12 mm bolt diameter; (e-h) Failure mode of
376 PFRP plate with $8d_b$ end distance with various thickness and diameter of bolts

377

378 A comprehensive study conducted by Coelho and Mottram [27] concluded that plate thickness (t),
379 end distance (e_1), and width of the plate (w) should be combined to formulate single parameter to
380 determine the complete characterisation of the PFRP connection. Therefore, in the present
381 research, a new parameter combining plate slenderness (w/t) and e_1/d_b ratio is proposed for
382 determining the appropriate connection geometry for achieving progressive damage and prior
383 warning before ultimate failure. A relatively similar approach was used by Rosner and Rizkalla
384 [19] for developing a failure criterion equation for the bearing strength of PFRP connections.
385 However, the equation by Rosner and Rizkalla [19] needs revision as the minimum e_1/d_b ratio
386 proposed was 5, whereas the results from the recent and present study indicated that a minimum
387 e_1/d_b ratio should not be less than 8 for achieving bearing failure. Therefore, the bearing stress
388 ($F/t*d_b$) and $(w/t)/(e_1/d_b)$ ratio were compared for determining the appropriate overall connection
389 geometric dimensions.

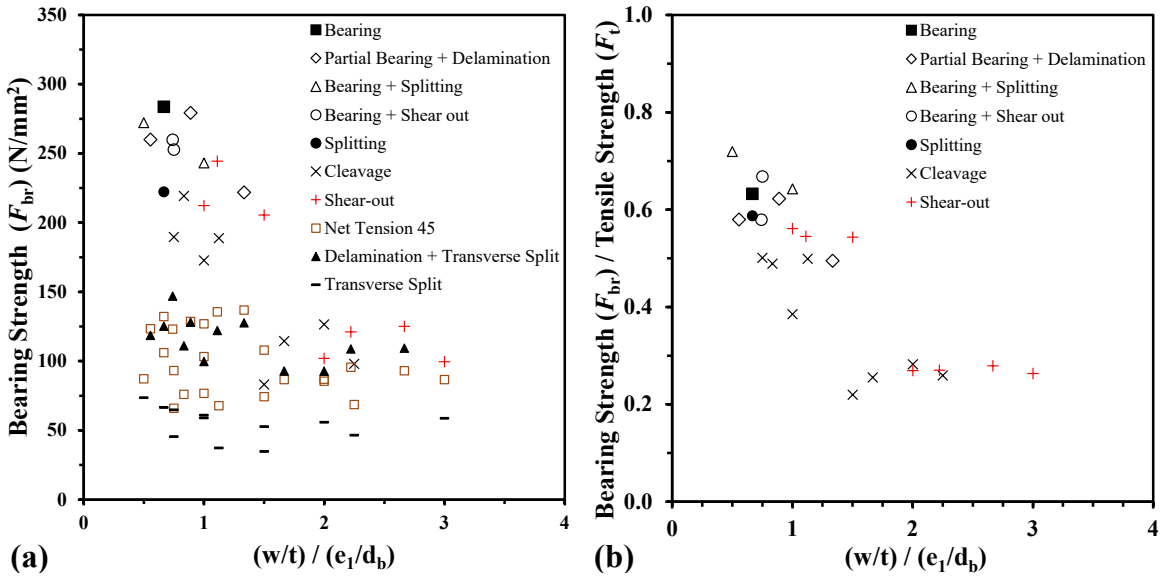

390

Fig. 7. (a) Variation of bearing strength of PFRP plate with $(w/t)/(e_1/d_b)$ ratio; (b) Bearing to tensile strength ratio with $(w/t)/(e_1/d_b)$ ratio

Figure 7a shows the variation of bearing strength (F_{br}) versus $(w/t)/(e_1/d_b)$ ratio and corresponding failure modes. The introduction of a new parameter resulted in $(w/t)/(e_1/d_b)$ ratios ranging from 0.5 to 3 for 72 test results. The representation of bearing strength with the new connection dimension ratio clearly shows the change in the failure mode trend with an increase in the $(w/t)/(e_1/d_b)$ ratio. The trend visibly shows that the undesirable failure modes such as cleavage, shear-out, transverse split, net tension 45˚, and delamination combined with transverse split exhibited low bearing stress in comparison with desirable failure modes (see Fig. 7a). It should also be noted that the failure modes of specimens with loading angle 45 degree and 90 degree are transverse split, net tension 45˚, and delamination combined with transverse split indicating underperformance as their bearing strength is less than 150 MPa (see Fig. 7a). It can also be noted that the variation in $(w/t)/(e_1/d_b)$ ratio from 0.5 to 3 (from larger width - higher end distance to narrow width - smaller end distance) for loading angle 45 degree and 90 degree did not influence the bearing strength and failure mode as shown in Fig. 7a. It indicates that the PFRP plates that are loaded not parallel to the unidirectional fibres requires much higher width and end distance [18]. For further investigation, the ratio to the bearing strength (F_{br}) and ultimate tensile strength (F_t) are used with varying $(w/t)/(e_1/d_b)$ ratios for specimens loaded parallel (0 degree) to the unidirectional fibres as shown in Fig. 7b. The comparison indicates that the specimens with a $(w/t)/(e_1/d_b)$ ratio less than 0.75 have failed in combination with bearing failure and higher F_{br}/F_t ratio. This indicates that the newly introduced connection dimension ratio is appropriately characterising the connections based on its dimensions. The Fig. 7b indicates that the bearing strength of the PFRP plates which achieved bearing failure is less than the ultimate tensile strength

of the plate, the maximum F_{br}/F_t ratio is 0.72. This result is not matching with the conclusions of Rosner and Rizkalla [18-19] whose F_{br}/F_t ratio is 1.84 for bearing failure. This incomparable result may be attributed to the difference in fibre weigh ratio and orientation reinforcements of the PFRP plates.

This investigation has addressed one of the six future research directions proposed by Coelho and Mottram [27] after a comprehensive review work. This article further exposed the following design implications that also leads to future research:

1. Current test results indicated that the fibre architecture of the PFRP plates (thickness of the bidirectional layer and ratio to the fibres in each direction) is one of the most influential parameters in connection behaviour as the failure mode is based on the thickness of the material.
2. The significant difference in F_{br}/F_t ratio with bearing failures indicating that the future connection characterisation strategies might consider including the material properties of the PFRP plate as an influential parameter.
3. The combination of failure modes requires a comprehensive research programme to get appropriate insight of the problem. Furthermore, a new guideline is required to define the failure mode with specific damage tolerance limit.

4. Conclusions

The mechanical behaviour of PFRP single bolted connections was studied experimentally. The main objective of this investigation was to determine the appropriate overall connection geometric dimensions to achieve the failure mode, which can exhibit larger deformation (progressive damage) before ultimate failure. It was also endeavored to verify the appropriateness of the minimum connection geometry limitations suggested in the existing design guidelines [12-15]. The connection tests were conducted with various parameters such as the thickness of the PFRP plate,

edge distance, end distance, width, bolt diameter, and angle of loading. The structural response of the connections is interpreted with the failure modes for the complete characterisation of the PFRP connections. The following conclusions can be drawn from the experimental results:

1. A total of ten different failure modes were observed in the tests including three new combined failure modes. The mechanics reasoning for such combined failure modes is elaborated. The interpretations and observations pertaining to the combined failure modes of PFRP connections indicate that the material characteristic limitations such as fibre orientation, the thickness of the bi-directional layers, and the percentage of fibres in the transverse direction shall be included as a variable in conjunction with the minimum geometric dimension requirement for connections.
2. The minimum edge distance (e_2) for the PFRP connection should be $2d_b$; this is consistent with the CNR 2008, EU 2016, and CEN/TS 2020 [12, 14, and 15] and inconsistent with the ASCE pre-standard [13]. It is determined that when the angle of loading is 45 or 90 degree with the direction of pultrusion, the PFRP plate has less strength and exhibit undesirable failure mode.
3. The bearing failure with progressive damage was achievable only when the end distance (e_1) was equal to $8d_b$. This result is inconsistent with the recommended minimum geometric dimension limitations of the current standards [12-15], which suggest a minimum e_1/d_b ratio of 4. Relatively similar ($e_1 \geq 8d_b$) recommendations were proposed in the recent study [16].
4. Finally, a new parameter combining plate slenderness (w/t) and (e_1/d_b) ratios is proposed for the complete characterisation of the PFRP connections. The comparison of the $(w/t)/(e_1/d_b)$ ratio with the failure modes indicates that most of the FRP connections with a $(w/t)/(e_1/d_b)$ ratio less than 0.75 have failed in combination with bearing failure with a warning.

However, the above recommendations are applicable for the $(w/t)/(e_1/d_b)$ ratio of 0.5 to 3 and regard to the failure modes summarised. Future research may be focused on combining the fibre orientations, volume fractions, and layer thickness with the minimum geometric dimension limitations for connections.

Acknowledgements

The research work presented in this paper was supported by the Research Grants Council of the Hong Kong Special Administrative Region, China – Theme-based Research Scheme (Project No. T22-502/18-R). The authors would like to thank the Industrial Centre of The Hong Kong Polytechnic University for facilitating the sample preparation and testing work. The authors would like to acknowledge the efforts of Mr. David Leung for his assistantship for FRP specimen preparation.

References

[1]. Wu, C., Tian, J., Ding, Y. and Feng, P., 2022. Axial compression behavior of pultruded GFRP channel sections. Composite Structures, 289, p.115438.

[2]. Feng, P., Li, Z., Wang, J. and Liu, T., 2022. Novel joint for pultruded FRP beams and concrete-filled FRP columns: Conceptual and experimental investigations. Composite Structures, 287, p.115339.

[3]. Liu, T., Feng, P., Wu, Y., Liao, S. and Meng, X., 2021. Developing an innovative curved-pultruded large-scale GFRP arch beam. Composite Structures, 256, p.113111.

[4]. Qureshi, J., Mottram, J.T. and Zafari, B., 2015. Robustness of simple joints in pultruded FRP frames. Structures, 3, p. 120-129.

[5]. Coelho, A.M.G., Mottram, J.T. and Harries, K.A., 2015. Bolted connections of pultruded GFRP: Implications of geometric characteristics on net section failure. Composite Structures, 131, p.878-884.

[6]. Qureshi, J. and Mottram, J.T., 2014. Response of beam-to-column web cleated joints for FRP pultruded members. Journal of Composites for Construction, 18(2), p.04013039.

[7]. Nguyen, T.T., Chan, T.M. and Mottram, J.T., 2014. Lateral-torsional buckling resistance by testing for pultruded FRP beams under different loading and displacement boundary conditions. Composites Part B: Engineering, 60, p.306-318.

[8]. Nguyen, T.T., Chan, T.M. and Mottram, J.T., 2013. Influence of boundary conditions and geometric imperfections on lateral–torsional buckling resistance of a pultruded FRP I-beam by FEA. Composite Structures, 100, p.233-242.
[9]. Nguyen, T.T., Chan, T.M. and Mottram, J.T., 2015. Lateral–Torsional Buckling design for pultruded FRP beams. Composite Structures, 133, p.782-793.
[10]. Coelho, A.M.G., Mottram, J.T. and Harries, K.A., 2015. Bolted connections of pultruded GFRP: Implications of geometric characteristics on net section failure. Composite Structures, 131, p.878-884.
[11]. Lee, Y.G., Park, S.Y., Park, J.S., Nam, J.H., An, D.J. and Yoon, S.J., 2011. Structural behavior of PFRP connection with single bolt. In Proc 18th Int Conf Comp Material (ICCM18).
[12]. CNR. 2008. Guide for the design and construction of structures made of FRP pultruded elements, CNR - Advisory Committee on Technical Recommendations for Construction and National Research Council of Italy, CNR-DT 205/2007, Rome, 2008.
[13]. American Society of Civil Engineers (ASCE) 2010. Pre-standard for load & resistance factor design (LRFD) of pultruded fiber reinforced polymer (FRP) structures (Final).
[14]. European Union (EU). 2016. Prospect for new guidance in the design of FRP. EUR 27666. Publications Office of the European Union; Ispra (Italy), JRC99714.
[15]. CEN/TS 19101. 2020. Design of Fibre-polymer composite structures, Technical committee, European Commission.
[16]. Martins, D., Gonilha, J., Correia, J.R. and Silvestre, N., 2021. Exterior beam-to-column bolted connections between GFRP I-shaped pultruded profiles using stainless steel cleats. Part 1: Experimental study. Thin-Walled Structures, 163, p.107719.
[17]. Abd-El-Naby, S.F.M. and Hollaway, L., 1993. The experimental behaviour of bolted joints in pultruded glass/polyester material. Part 1: Single-bolt joints. Composites, 24(7), pp.531-538.
[18]. Rosner, C.N. and Rizkalla, S.H., 1995. Bolted connections for fiber-reinforced composite structural members: experimental program. Journal of materials in civil engineering, 7(4), p.223-231.
[19]. Rosner, C.N. and Rizkalla, S.H., 1995. Bolted connections for fiber-reinforced composite structural members: Analytical model and design recommendations. Journal of materials in civil engineering, 7(4), p.232-238.
[20]. Turvey, G.J., Cooper. C., 1995. Single bolt tension joint tests on pultruded GRP WF-section web and flange material, in: Proc. 10th International Conference on Composite Materials ICCM-10, Woodhead Publishing Ltd., Vancouver, 1995, p. 621–628.
[21]. Prabhakaran, R., Razzaq, Z. and Devara, S., 1996. Load and resistance factor design (LRFD) approach for bolted joints in pultruded composites. Composites Part B: Engineering, 27(3-4), p.351-360.
[22]. Turvey, G.J., 1998. Single-bolt tension joint tests on pultruded GRP plate—effects of tension direction relative to pultrusion direction. Composite structures, 42(4), p.341-351.
[23]. Yuan, R. L., Liu, C.J., 2000. Experimental characterization of FRP mechanical connections, in: Proc. 3rd International Conference on Advanced Composite Materials in Bridges and Structures ACMBS-3, The Canadian Society for Civil Engineers Montreal, p. 103–110.
[24]. Wang, Y., 2002. Bearing behavior of joints in pultruded composites. Journal of composite materials, 36(18), p.2199-2216.
[25]. Turvey. G.J., 2012. Failure of single-lap single-bolt tension joints in pultruded glass fibre reinforced plate, in: Proc. 6th International Conference on Composites in Construction Engineering (CICE), Rome, 2012, Paper 08.089.

[26]. Turvey, G.J., Godé. J., 2012. An experimental investigation of the tensile behaviour of single-lap bolted joints in pultruded GFRP plate, in: Proc. FRP Bridges Conference, London, p. 77–91.
[27]. Coelho, A.M.G. and Mottram, J.T., 2015. A review of the behaviour and analysis of bolted connections and joints in pultruded fiber reinforced polymers. Materials & Design, 74, p.86-107.
[28]. ASTM. 2014. Standard test method for tensile properties of polymer matrix composite materials. ASTM D3039/D3039M. West Conshohocken, PA: ASTM.
[29]. Wu, C., Feng, P. and Bai, Y., 2015. Comparative study on static and fatigue performances of pultruded GFRP joints using ordinary and blind bolts. Journal of Composites for Construction, 19(4), p.04014065.
[30]. Selvaraj, S. and Madhavan, M., 2020. Design of steel beams strengthened with low-modulus CFRP laminates. Journal of Composites for Construction, 24(1), p.04019052.
[31]. ASTM. 2015. Standard test methods for constituent content of composite materials. ASTM D3171. West Conshohocken, PA: ASTM.
[32]. Selvaraj, S. and Madhavan, M., 2019. Strengthening of laterally restrained steel beams subjected to flexural loading using low-modulus CFRP. Journal of Performance of Constructed Facilities, 33(3), p.04019032.
[33]. A.S. Mosallam, Design guide for FRP composite connections, ASCE Manuals and Reports on Engineering Practice No. 102, American Society of Civil Engineers, Reston, 2011, ISBN: 978-0-7844-0612-0.
[34]. Bank, L. C. 2006. Composites for construction: Structural design with FRP materials, Wiley.
[35]. Strongwell. Strongwell design manual - EXTREN® and other proprietary pultruded products. Bristol (VA): Strongwell; 2013.
[36]. Lee, Y.G., Choi, E. and Yoon, S.J., 2015. Effect of geometric parameters on the mechanical behavior of PFRP single bolted connection. Composites Part B: Engineering, 75, p.1-10.